by C. M. Mate

Force microscopy studies of the molecular origins of friction and lubrication

The atomic force microscope (AFM) has become a valuable instrument in recent years for studying the atomic and molecular origins of friction and lubrication. This paper reviews the effort in our laboratory using force microscopy to develop a molecular-scale understanding of friction and lubrication. Among the topics covered in this paper are 1) the nanomechanics and adhesive forces of lubricated and unlubricated surfaces, 2) the observation of atomic-scale features and their effect on the friction force for AFM tips sliding over graphite and mica surfaces, and 3) the effect of lubricating surfaces with bonded and unbonded perfluoropolyether polymers and with water molecules adsorbed from the ambient. Many of the descriptions developed using macroscopic continuum mechanics analysis are still applicable to these atomicscale contact zones. However, a complete interpretation of the results requires

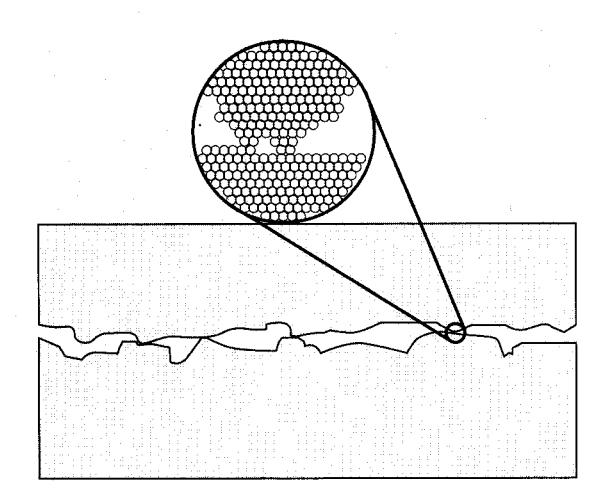
incorporating descriptions of the atomic and molecular processes into the continuum mechanics analysis.

Introduction

For many years, researchers from diverse disciplines (e.g., physics, chemistry, materials science, and engineering) have studied the phenomena of friction, lubrication, and wear that make up the field of tribology. Only recently has a common approach been developed for tying together these diverse avenues of research: the development of a molecular-scale understanding of friction, lubrication, and wear. All of these tribological phenomena have their origins at the atomic and molecular levels with the formation and breaking of chemical bonds, the motion of atoms and molecules against one another, and the dissipation of energy in the form of heat and electronic excitations. Owing to their common molecular origins, molecular-scale concepts developed for one tribological system should be readily applicable to new situations,

^eCopyright 1995 by International Business Machines Corporation. Copying in printed form for private use is permitted without payment of royalty provided that (1) each reproduction is done without alteration and (2) the Journal reference and IBM copyright notice are included on the first page. The title and abstract, but no other portions, of this paper may be copied or distributed royalty free without further permission by computer-based and other information-service systems. Permission to republish any other portion of this paper must be obtained from the Editor.

0018-8646/95/\$3.00 © 1995 IBM



Flaure

Schematic diagram of two contacting rough surfaces. The inset illustrates the contact of several atomic microasperities.

helping to tie together what may at first appear to be diverse phenomena.

Since its invention in 1986, the atomic force microscope (AFM) [1] has become an important instrument in determining the molecular origins of tribology, since it can control and image the results of mechanical events involving as little as a single atom. This paper is a review of the efforts of our laboratory in using atomic force microscopy to elucidate the molecular origins of friction and lubrication.

Theory of contacts

Much of our understanding of what happens at the atomic and molecular levels when two surfaces touch is an extension of concepts already developed using macroscopic continuum mechanics analysis. Consequently, a useful starting point for understanding contacts at the atomic scale is to review briefly the continuum mechanics theory of contacts. Because most surfaces of solid materials have some degree of roughness, when two surfaces touch, contact occurs predominately at the summits of the surface roughness, as illustrated in Figure 1. When the surfaces are first brought together, the contacting asperities initially deform elastically. When an individual contact is modeled as a perfectly smooth sphere on a flat surface, elastic deformation occurs according to Hertz's classical equations, with the radius a of the contact zone given by

$$a = \left[\frac{3LR}{2} (k_1 + k_2) \right]^{1/3}, \tag{1}$$

where R is the asperity radius, L is the load force pushing the two surfaces together, and k_1 and k_2 are the elastic constants of the two materials, with $k=(1-\nu^2)/E$, where E is Young's modulus and ν is the Poisson ratio. For this type of elastic contact, known as Hertzian contact, the contact area πa^2 is proportional to $L^{2/3}$.

For surfaces with substantial roughness, such as those shown in Figure 1, contact occurs at many points. The case of many contacting asperities has been studied by Greenwood and co-workers [2–4], who analyzed elastic, Hertzian contact of many spherically shaped microasperities for a statistical distribution of heights of the microasperities. This analysis shows that more microasperities are brought into contact as the load increases, and that the number of contact points is proportional to load. Further, the average contact area of the individual contact points is fairly independent of load. Consequently, for the situation of many asperities contacting elastically, the total contact area is proportional to load.

As the force on the contacting materials is increased, the contact pressure on individual microasperities increases until the elastic limit of the softer material is exceeded. Plastic deformation increases the area of contact until the contact pressure in the material is less than the yield pressure P_y . The area of contact A_c from plastic deformation due to a load force L is approximately $A_c = (L/P_y)$. Thus, the area of contact from plastic deformation is proportional to load, just as is the case for the elastic deformation of multiple asperity contacts.

The previous discussion considered only what occurs at the contacting asperities when two materials are brought into static contact. If materials slide against each other, a friction force opposes this motion. Following Bowden and Tabor [5], the friction force can be divided into two parts: a plowing term for the force needed to plow the asperities of the harder material through the softer material, and a shearing term for the force needed to shear the contacting junctions. If s is the shear strength of the contact points, the friction force for the shearing term is $F = A_c s$. Since the contact area A_c is proportional to load both for elastic and plastic deformation when multiple asperity contacts are involved, the friction force is generally proportional to the load force (Amontons' law). In particular, for plastic deformation,

$$F = A_{c}s = \frac{L}{P_{y}}s = \mu L, \tag{2}$$

where $\mu = (s/P_y)$ is the coefficient of friction. This simple description, which ignores what is happening on the atomic

level, provides a simple expression for friction. The atomistic mechanisms of friction, however, are buried in the terms s for the shear strength and P_y for the yield pressure. To properly understand these terms, one requires understanding at the atomic level.

A simple atomic-level model [6-8] of the shear strength s which must be overcome to initiate sliding between two surfaces separated by a molecularly thin liquid film is as follows: Before sliding can commence, the two surfaces must be separated in the direction normal to the interface by a small amount ΔD so that the liquid molecules have enough room to slide over the atoms on the solid surfaces the small distance Δd corresponding to an atomic dimension. If the force of adhesion between the two surfaces is F_{ad} , the energy required to separate the two surfaces to initiate sliding is $\Delta D \times F_{\rm ad}$, which is some small fraction ε of the total adhesion energy $2\gamma A$. If we assume that the external normal force contribution is negligible in comparison with the internal adhesive force and that all of the energy used to separate and move the surfaces the distances ΔD and Δd is dissipated as heat,

$$\Delta d \times F = \Delta D \times F_{\rm ad} = (2\gamma A)\varepsilon,$$
 (3)

which leads to

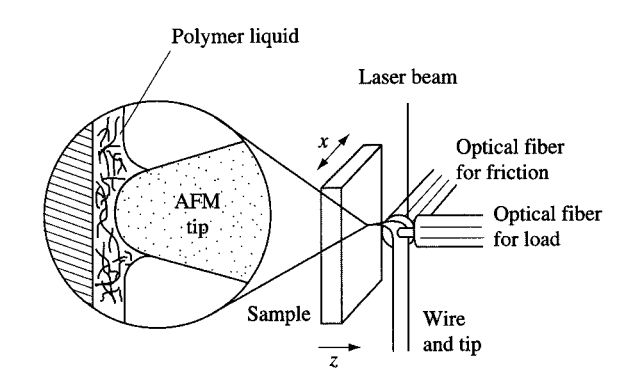
$$s = \frac{F}{A} = \frac{2\gamma\varepsilon}{\Delta d} \tag{4}$$

for the shear strength which must be overcome. Assuming that $\gamma = 25 \times 10^{-3} \text{ J/m}^2$, a typical value for a hydrocarbon surface, and that 10% of the surface energy is lost each time the surfaces move an atomic distance, i.e., $\varepsilon \sim 0.1$ and $\Delta d \sim 1$ Å, then $s \sim 5 \times 10^7$ N/m, which compares well with surface force apparatus experimental results for shearing one layer of hydrocarbon between two mica surfaces [7, 8].

This model is often referred to as the cobblestone model [7, 8], since the motion is analogous to pushing a cart over a cobblestone road, where a certain amount of lateral force is needed to raise the wheels of the cart against the force of gravity to start the cart moving. Energy is dissipated as heat (i.e., phonons, acoustic waves, etc.) every time a wheel hits the next cobblestone. In this analogy, the wheels represent the liquid molecules, which settle into a low-energy configuration among the cobblestones (the solid surface atoms) when the cart is at rest.

Force microscopy instrumentation

In force microscopy, forces acting on a single asperity, in the form of a sharp tip, are measured by mounting the tip at the end of a compliant cantilever with a known spring constant. The force on the tip is determined by measuring the deflection of the cantilever and multiplying it by the



Flaure 2

Schematic diagram of the region around the tip, sample, and optical fibers of the force microscope used in the IBM Almaden Research Laboratory. Inset illustrates how a meniscus forms around the tip when it contacts a liquid lubricant film.

spring constant. The key to AFM is to measure the force on the tip while maintaining the positional accuracy of the tip to better than an atomic dimension. To do this, cantilever deflections smaller than an ångstrom must be measured. In the first AFM, this was accomplished by measuring the tunneling current between an STM tip and the back of the cantilever [1]. Tunneling detection eventually proved to be unreliable, so it has been superseded by the optical detection methods of optical interference [9, 10] and beam deflection [11, 12].

The force microscope used in our laboratory is shown schematically in **Figure 2.** The force microscope is similar in principle to the one originally described by Rugar et al. [10] and uses two orthogonal optical fibers for measuring independently the components perpendicular (load force) and parallel (friction force) to the sample surface. The force microscope cantilever is constructed by bending a thin tungsten wire at a right angle and etching the end to a sharp point to form a tip. The perpendicular and parallel deflections of the wire are measured by optical interference between the laser light reflected off the back and side of the wire and the laser light reflected internally off the ends of the optical fibers.

Nanomechanics and adhesive forces determined by force microscopy

Force microscopy is an excellent instrument for studying the elastic properties and surface forces that occur at ultrasmall contact areas. These properties are typically studied by measuring the load force on the tip as a



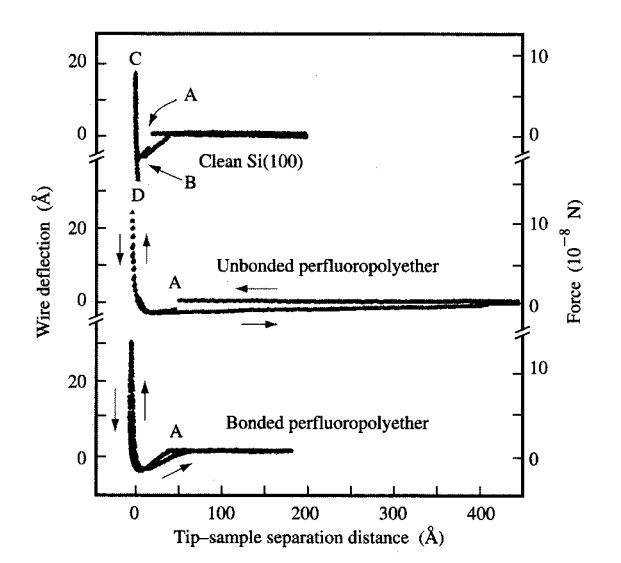


Figure 3

Load-force-vs.-distance curves comparing the behavior of clean Si(100), a 40-Å-thick unbound, liquid perfluoropolyether polymer film on Si(100), and a 15-Å-thick bonded perfluoropolyether polymer film on Si(100). A negative direction indicates an attractive force. From Reference [13], reproduced with permission.

function of tip-sample separation distance, i.e., force-vs.distance curves. Figure 3 shows the load force acting on a tungsten tip as silicon wafers, prepared with and without perfluoropolyether lubricant films, are brought into contact with the tip and then withdrawn. When the tip is far away from the sample, the force is near zero. When the tip contacts the top of contaminant molecules on the nominally clean silicon surface, a sudden attractive force is observed at point A in the top curve. Similarly, a sudden force is observed in the middle curve when the tip touches the top of the liquid lubricant film. The sudden attractive force is due to the formation of a capillary meniscus composed of liquid lubricant molecules, as illustrated in Figure 2 [13, 14]. For the bonded polymer film (bottom curve, Figure 3), only a gradual increase in the attractive force is observed, since the bonded molecules are unable to migrate to the tip-sample contact zone to form a liquid meniscus.

The force on the tip turns repulsive after the tip has pushed through the liquid film or compressed those molecules trapped underneath the tip. The slope of the repulsive force-vs.-separation-distance curve gives the stiffness of the near-surface region in the contact zone. For the clean silicon wafer, the stiffness is 110 N/m at point B in Figure 3, rising quickly to 350 N/m at point C. The

stiffness S is related to the elastic properties and size of the contact zone by $S = kaE^*$, where k is a geometric factor between 1.9 and 2.4, a is the radius of contact, and E^* is the composite of the elastic modulus of the tip and sample [15]. Consequently, the measured value of the stiffness can provide an estimate of either the contact radius or the elasticity, if one of these values is known or can be approximated. For example, assuming a value of $2 \times 10^{11} \text{ N/m}^2$ for E^* for the clean silicon wafer provides an estimate of 3 Å for the contact radius when the tip first comes into repulsive hard-wall contact, indicating a contact zone of atomic dimensions.

Burnham et al. [16, 17] have also used force microscopy to study the surface stiffness for a variety of tip/sample combinations: gold/nickel, tungsten/gold, tungsten/elastomer, tungsten/graphite, diamond/graphite, and diamond/diamond. They have observed that the higher the elasticity of the tip and sample materials, the stiffer the contact zone. For samples made of gold, the softest material studied by Burnham et al., indentation of the gold surface was observed even at the very small loads used.

When the tip and sample are separated from contact, the solid-solid adhesive forces must be overcome, which occurs at point D for the clean silicon surface in Figure 3. From the other force-vs.-distance curves in Figure 3, one can see that the addition of a low-surface-energy film (the perfluoropolyether polymer film has a surface energy of only 24 dynes/cm) reduces the maximum adhesive force observed by a factor of 2 to 3 from that of a clean silicon surface. The solid-solid adhesive force due to van der Waals interaction is directly related to the sample surface energy by $F_{ad} = 4\pi R(\gamma_t \gamma_s)^{1/2}$, where R is the tip radius and γ , and γ are the surface energies of the tip and sample surfaces [18]. Burnham et al. [19] have systematically studied the correlation between solid-solid adhesive forces and sample surface energies and found larger adhesive forces for samples with higher surface energies; however, the magnitude of the force was about a factor of 10 lower than that predicted by $F_{\rm ad} = 4\pi R(\gamma_{\rm t}\gamma_{\rm s})^{1/2}$. The lower-thanpredicted adhesive forces are attributed to the effective tip radius being much smaller than the measured macroscopic radius R because of the presence of small microasperities at the end of the tip.

As the sample is further withdrawn in Figure 3, the attractive forces gradually decrease as the tip tries to break free from the molecules that gathered around the tip during contact. This extends the farthest out for the unbonded perfluoropolyether film, where a large number of liquid molecules have migrated to the tip-sample contact zone to form a liquid meniscus around the tip, which now must be extended to the breaking point before the force on the tip can return to zero [14].

Atomic-scale friction

• Graphite and mica

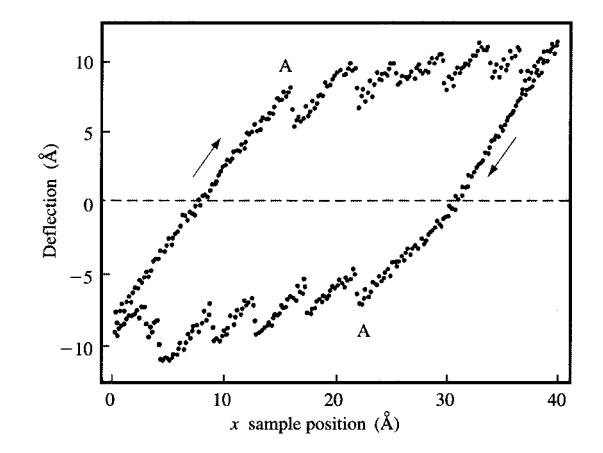
In 1987, the author and his co-workers at the IBM Almaden Research Center used AFM to observe atomicscale friction for a tungsten tip sliding on the basal plane of a graphite surface [9] and the following year on muscovite mica [20], both layered compounds. Figure 4 shows the wire deflection parallel to the sample surface as a mica sample is moved first in one direction, then in the reverse direction, underneath the tungsten tip to generate a "friction loop." Initially, the tip moves with the sample until, at point A, the cantilever wire exerts enough force on the tip to overcome the static friction and the tip starts to slip across the surface. The sliding process is not uniform, but instead the tip slips a distance corresponding to the size of the unit cell of the hexagonal SiO, layer in the cleavage plane of muscovite mica, i.e., an atomic-scale stick-slip process. Similar atomic-scale slips are observed in the friction loops for tips sliding across the basal plane of graphite [9]. That these slips have the periodicity of the sample surface can be seen in Figure 5, which shows a map of the deflection of the wire cantilever parallel to the surface as the graphite sample is rastered underneath it. The periodicity of the graphite lattice is clearly visible.

The remarkable aspect of the atomic-scale stick-slip process on graphite and mica is that it has been observed at loads as high as 10^{-4} N. At these loads, the contact area for the tungsten tip on the graphite surface is estimated to be greater than 10^6 Å², indicating that a large number of tip atoms are in contact with the sample surface. Even though each tip atom would be expected to experience a periodic friction force as it slides over the graphite surface, the forces would be randomly out of phase with one another because of the inhomogeneous and disordered nature of the tungsten tip surface, which should result in only a small net periodic component of the friction force on the tip. Instead, a very large periodic friction force is implied by the large (2500 N/m) spring constant used for Figure 5.

Other surfaces

Since the initial observation of atomic-scale friction on graphite and mica, there have been several reports of atomic-scale friction on nonlayered compounds. For example, Akamine et al. [21] have observed atomic-scale stick-slip motion on a gold (111) surface at fairly high loads (>10⁻⁷ N). Meyer and Amer [12] have observed the effect of atomic steps on friction for a Si_3N_4 tip sliding over a clean NaCl crystal surface in ultrahigh vacuum at a load of 10^{-8} N.

One of the clearest cases of atomic-scale friction on a nonlayered compound is that found by Germann et al. [22]



Elitabilities

Typical friction loop of the wire cantilever deflection parallel to the sample surface for a force microscope tip sliding across a mica surface. The wire spring constant is 100 N/m. From Reference [20], reproduced with permission.

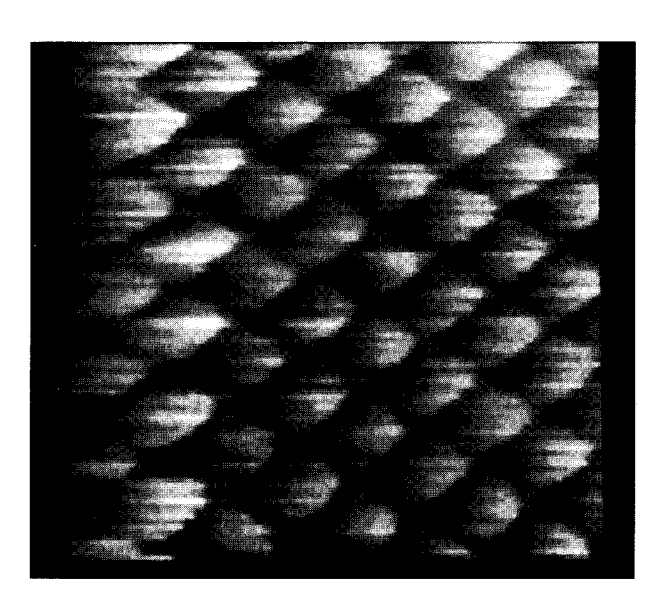


Figure:

Frictional force, indicated by brightness, as a function of sample position, while a tip was dragged from left to right across a 20-Å \times 20-Å area of a graphite sample. From Reference [9], reproduced with permission.

for a diamond tip sliding against hydrogen-terminated diamond (111) and (100) in ultrahigh vacuum. Their friction images on the (100) surface show rows along the $\langle 021 \rangle$ direction spaced by a single lattice constant along the $\langle 001 \rangle$

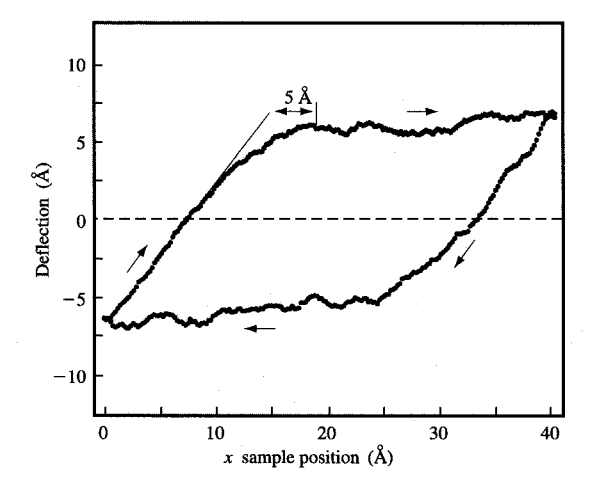


Figure 6

Typical friction loop of the wire cantilever deflection parallel to the sample surface for a force microscope tip sliding across the native silicon oxide surface of a Si(100) wafer. The wire spring constant is 90 N/m

direction, a pattern consistent with a 2×1 reconstruction. The contact radius for these images, assuming elastic Hertzian contact, is estimated to be less than 1.6 nm, indicating a contact zone of near-atomic dimensions. Germann et al. propose that the deflection of individual bonds is involved in the friction mechanism.

• Models of atomic-scale friction

Obviously, the effect of atomic-scale features on the friction force is most easily observed when the contact zone is of atomic dimensions, i.e., less than a few nanometers across. This occurs when the loads on the tip are $<10^{-8}$ N for the stiffest materials, such as diamond, and at correspondingly smaller loads for less stiff materials. Consequently, much of the theoretical work presented in the literature has been for single-atom tips, which are intended to model a contact zone consisting of a small number of atoms (for example, [23–27] for atomic-scale friction on graphite).

Frequently, atomic-scale features are observed on the friction force at larger loads where the contact zone consists of many surface atoms. In this case, the mechanism by which the tip starts to slip or slide across the surface is not as simple as it first appears because of the process known as "incipient sliding" [28]. The load pressure is not uniform across the contact zone, but rather is highest at the center and goes to zero at the edge of the zone. Also, the lateral force from the cantilever exerts a

nonuniform shear stress on the contact zone which is lowest at the center and diverges at the edge of the contact zone if no slippage occurs within the zone. Consequently, the shear stress at the perimeter of the contact zone exceeds $\mu p(r)$ for r > some critical radius [$\mu =$ static friction coefficient, p(r) = load pressure as a function distance away from the center of the contact zone]. Outside the critical radius, the contacting surfaces undergo microslippage. As the lateral force is increased, the annulus of microslippage grows toward the center of the contact zone, until just before the onset of gross sliding, the entire contact zone has undergone microslippage except for a single point at the center. Evidence of this "incipient sliding" can be seen in the friction loop shown in Figure 6 for a tungsten tip on a native SiO, layer on a Si(100) surface. When the tip and sample move together before sliding, the curve bends over substantially before smooth sliding begins. This bending appears to follow the 2/3 power dependence on lateral force expected during incipient sliding. The 5-Å difference observed in Figure 6 between the solid line and the onset of uniform sliding is approximately equal to the maximum amount of microslippage that occurs in the contact zone before the onset of gross sliding. It would be difficult to observe atomic-scale friction features if the amount of microslippage were much greater than an atomic dimension. The microslippage is minimized by working at small loads, which also reduces the size of the contact zone, and by using stiff tip and sample materials.

For layered compounds such as graphite or mica, a more likely explanation for the large periodic friction force needed to cause the observed atomic-scale stick-slip motion observed in Figures 4 and 5 is that a small graphite or mica flake becomes attached to the end of the tip. A similar mechanism was originally suggested by Pethica [29] to explain STM images of graphite surfaces. As the flake is dragged over the surface, the flake atoms coherently go in and out of phase with the surface lattice, resulting in a friction force having the periodicity of the surface lattice and proportional in magnitude to the size of the flake.

Lubrication

• Liquid lubricant films

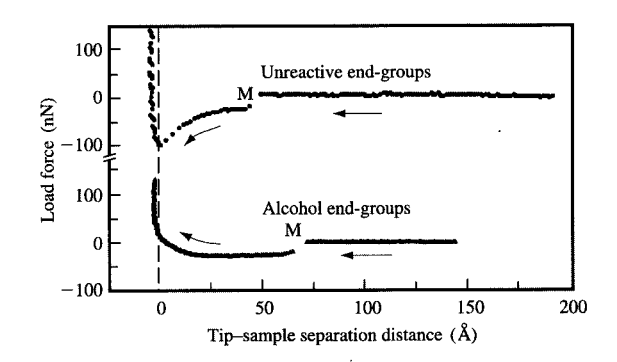
Most lubricants can be classified as either liquid or solid depending on whether they can support a shear force in a real tribological situation. This section discusses what has been learned by force microscopy on how liquid polymers and adsorbed water films lubricate at the molecular level, while the following section discusses solid polymer lubricants.

First, we look at the importance of end-groups to the lubricating properties [30]. Figure 7 shows the force-vs.-distance curves as a tip is brought into contact with silicon

wafers covered with two slightly different liquid polymer films. The polymer films are both perfluoropolyethers frequently used as lubricants in high-technology applications such as computer disk drives. These polymers, Fomblin® Z-03 and Fomblin Z-Dol from Montefluos, have the same linear polymer backbone— $(OC_2F_4)_q(OCF_2)_p$ —and differ mainly in that Fomblin Z-Dol has reactive alcohol end-groups at both ends of the linear polymer chain, while Fomblin Z-03 has only unreactive CF_3 end-groups.

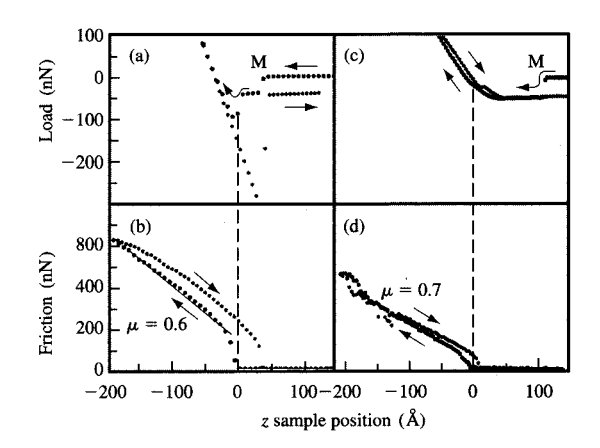
In Figure 7, a sudden attractive force is observed at point M due to the formation of a liquid meniscus when the tip comes in contact with the top of the liquid film, which was also seen for the force-vs.-distance curve in the center of Figure 3 and is illustrated in Figure 2. For the liquid polymer with unreactive end-groups, the normal force becomes increasingly more attractive for decreasing tip-sample separation distances less than 25 Å. When hard-wall contact is reached, the normal force quickly turns repulsive. The attractive force on the tip at these small separation distances is the sum of the capillary force from the liquid meniscus and solid-solid attraction, most likely van der Waals attraction, mediated by the liquid polymer. For the liquid polymer with alcohol end-groups, the normal force is very different for separation distances less than 25 Å. At these distances, the net force becomes increasingly less attractive. The attractive forces on the tip are still present, but are counteracted by a repulsive force associated with the alcohol end-groups. The repulsive force would come first from the compression of the molecule underneath the tip, followed by the force needed to overcome the hydrogen bonding of the alcohol endgroups to the silicon oxide surface so as to squeeze out the lubricant molecules from between the two surfaces. Therefore, a major effect of the alcohol end-groups is to increase dramatically the load or contact pressure that a liquid lubricant film can support before solid-solid contact. An extra load force of 100 nN is needed to make hardwall contact for polymer film with alcohol end-groups in comparison to the polymer film with neutral end-groups. If the extra 100-nN load were spread out over 104 Å2, it would imply that a contact pressure of the order of 1 GPa is needed to squeeze out the molecules with alcohol end-groups.

Friction experiments with force microscopy show that the alcohol end-group polymer lubricants maintain their load-bearing capacity during sliding. In these experiments, the sample is moved back and forth in the x direction to generate friction loops, such as those shown in Figures 4 and 6, while the load on the tip is slowly increased and then decreased by moving the sample in the z direction. Figure 8 shows the average load and frictional force during sliding as a function of z sample position. As the sample approaches the tip, contact with the lubricant occurs at point M, but the friction is negligible for both films until



E (TITES)

Inward load-force-vs.-distance curves; upper curve is for a perfluoropolyether polymer film with unreactive end-groups, while the lower curve is for a perfluoropolyether polymer film with alcohol end-groups. From Reference [30], reproduced with permission.



Flaure 8

Friction and load force as a function of z sample position for 30-Å-thick films on Si(100) of unbonded liquid polymer (a), (b) with unreactive end-group, (c), (d) with alcohol end-groups. Each data point represents the average during sliding over one friction loop. From Reference [30], reproduced with permission.

the tip pushes far enough into the liquid film to make hard-wall contact. For the nonalcohol-end-group polymer, the load force during sliding becomes more attractive just before hard-wall contact and, for the alcohol-end-group polymer, more repulsive, in the same manner observed in Figure 7 where no sliding occurs. Before hard-wall contact takes place, shearing of the liquid film occurs, while after hard-wall contact, solid-solid shearing occurs. The

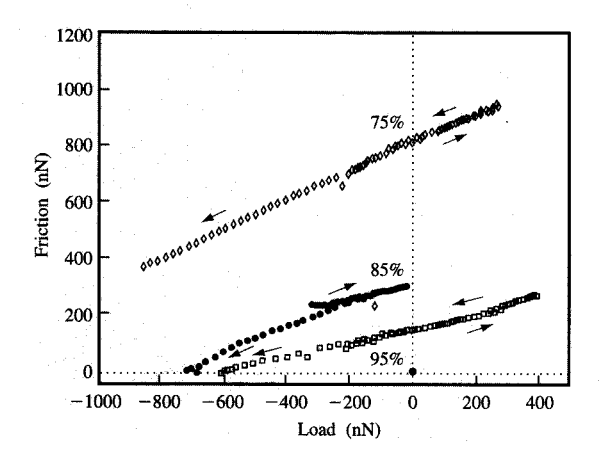


Figure 9

Friction-vs.-load at different humidities on a silicon oxide surface on a Si(100) wafer. Each data point represents the average during sliding over one friction loop. The arrows indicate whether the load is increasing or decreasing. From Reference [31], reproduced with permission.

transition between the two regimes is very sharp, requiring a change in separation distance of less than the diameter of a linear polymer chain (~7 Å).

When the sample is withdrawn, an adhesive force of almost 300 nN must be overcome to break sliding contact on the nonalcohol polymer film, while for the alcoholend-group polymer, almost no adhesive force must be overcome to break friction contact. The low adhesion is attributed to the alcohol end-groups forcing their way back into the sliding interface and separating the surfaces at low loads in order to reestablish hydrogen bonding with the oxide surfaces of the tip and sample.

The previous example shows the dramatic effect that OH groups can have on the lubrication properties of a molecule. Water is another molecule that interacts strongly with surfaces and other molecules via hydrogen bonding of OH groups. Because of its abundance and particular chemical properties, water is an important adsorbant molecule known to have a dramatic effect on tribological properties of surfaces. In particular, water vapor can condense around contacting asperities at moderate to high humidities. Figure 9 shows the results of AFM friction-vs.-load experiments at high humidities for a tungsten tip sliding on clean silicon wafers [31]. For low to moderate humidities (<75%), no effect of humidity was observed on friction.

Even at these ultralow loads, friction is observed to be linear with load, implying that the actual contact occurs through multiple asperity contacts as discussed in the section on the theory of contacts. The slopes of the linear friction-vs.-load curves provide the friction coefficients μ , and extrapolating the curves to zero friction force yields an estimate of the adhesive forces during sliding. The strong dependence of the friction properties on the humidity is clearly apparent: μ drops from 0.5 to 0.25, and the adhesive force drops from 1.5 μ N to 0.7 μ N. The reduction of the friction coefficient with increasing humidity is interpreted to result from the increasing water partial pressure pushing unbound water molecules into the microasperity contact junctions, reducing the shear strength of the junctions. A similar reduction in shear strength with increasing humidity has been observed during shearing of mica surfaces in the surface force apparatus (SFA), which was attributed to water displacing organic contaminants and reducing the true area of contact [7].

It is valuable to compare the force microscopy results for liquid films with those obtained using the surface force apparatus. In SFA experiments, liquid films are sheared between two parallel, molecularly smooth mica surfaces with a contact zone typically 100 μ m across. Consequently, a large number of molecules are confined to an exceptionally narrow space. For films less than 50 Å thick, results of Hu et al. [32] indicate that this type of confinement leads to an increase in collective motions of the molecules with decreasing film thickness, resulting in the effective viscosity of the films being dramatically enhanced by many orders of magnitude. To interpret these results within the cobblestone model, the thicker the film, the easier it is for the liquid molecules ("cart wheels") to move over the surface atoms, so that two surfaces move a much smaller distance ΔD normal to the interface, and a much smaller fraction ε of the surface adhesion energy is lost during sliding. For films thinner than about five molecular layers, the parallel nature of the two surfaces leads to layering of the molecules between the surfaces. When these thinnest films are sheared, solid-like response is typically observed [33–35].

In contrast, in the force microscopy experiments discussed here, liquid polymer films can exhibit negligible shear force for separation distances as small as a few chain diameters with an effective viscosity no more than a few orders of magnitude greater than the bulk viscosity. This difference in behavior is most likely related to the vastly different geometries of the SFA and force microscopy experiments. For force microscopy, the geometry is one of a spherically shaped surface, rough on the molecular scale, sliding against a smoother flat surface. The sharp radius of curvature and the rough morphology of the tip surface make it difficult for the polymer molecules to form layers between the sliding surfaces. Also, the lateral dimension of the contact zone for the tip is more than 10^3 times smaller than for the SFA experiments. Consequently, the

molecules need travel only a short distance to escape from underneath the sliding tip. Within the cobblestone model, this would correspond to the cart wheels being able to move off to the side of each cobblestone rather than being raised over them to initiate sliding.

• Solid polymer lubricants

Polymers bonded to surfaces are an important class of lubricant. Since bonded polymer molecules are not free to move across the surface, they usually act like a solid when subjected to a shear force. However, if the bonded polymers are given enough room for the polymer backbone to move out of the way of the shearing surface, this polymer film can act like a liquid film at low loads and like a solid film when compressed at high loads. Figure 10 shows the friction and load forces from sliding on such a bonded polymer surface [30]. This bonded polymer surface was formed by heating a silicon wafer covered with Fomblin Z-Dol at 150°C for one hour in order to react the alcohol end-groups with the hydroxyl groups on the silicon oxide surface. At point M a slight attractive load force is observed when contact is made with the top of the bonded polymer layer. As the tip penetrates the film, increasing the area of contact, the attractive force increases gradually because of the increase in attractive van der Waals interaction between the molecules and the tip. As was also the case for the unbonded liquid polymers, no significant friction is observed until hard-wall contact is made. So, even though the ends of the polymer are rigidly attached to the substrate, the backbone of the polymer apparently has enough flexibility to offer little resistance to the sliding tip except when rigidly compressed between the two surfaces.

In Figure 10, the initial friction coefficient, $\mu=0.3$, is about half that for the unbonded liquid films. The lower friction indicates that significantly more molecules are trapped between the rubbing surfaces than for the unbonded polymer. With repeated traversals of the sliding tip, these attached molecules eventually wear away, and the friction coefficient increases with increasing load. As the sample is retracted, the friction is substantially higher than on the inward approach. Further evidence for wearing away of the bonded polymer comes from repeating the sliding experiment in the same spot. In this case, the friction starts at a higher value than during the first experiment and has an even higher value when the sample is retracted.

Polymer films where the polymer chains have very little room to move act like solid films in that they provide resistance to a shear stress. Langmuir–Blodgett films deposited on solid surfaces are the films of this type most frequently studied by friction force microscopy. In an elegant series of experiments [36–38], the group at the University of Basel has studied the friction force on a tip

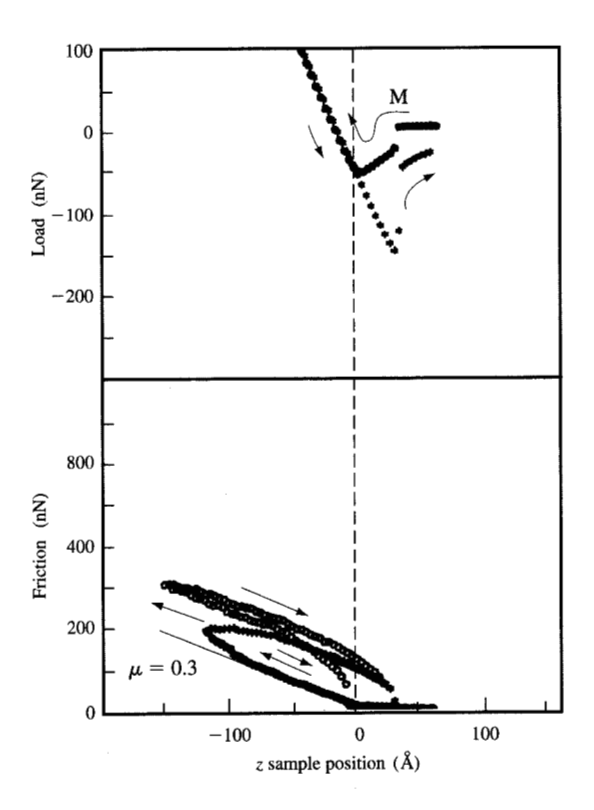


Figure 10

Friction and load force as a function of z sample position for a film of bonded polymer (Fomblin Z-Dol) on a Si(100) wafer. From Reference [30], reproduced with permission.

sliding on mixed Langmuir-Blodgett films on silicon wafers, which allow for side-by-side comparison of the frictional properties of different L-B films. For example, at a load of a few nanonewtons, domains of L-B film with hydrocarbon chains exhibited friction forces a factor of 10 less than the underlying silicon wafer substrate and a factor of 4 less than domains of L-B film with fluorocarbon chains [36]. The higher friction on the fluorocarbon domains compared to the hydrocarbon domains is attributed to a lower elasticity modulus of the fluorocarbon film, which results in a larger contact area [37, 38].

Conclusions

With the invention of the atomic force microscope, it is now possible to study friction and lubrication of atomic-size contact zones. Atomic-scale features have been observed in our laboratory on the friction force for tips sliding over graphite and mica surfaces and on other types of surfaces in other laboratories. The effect of lubricating surfaces with bonded and unbonded perfluoropolyether

polymers has also been studied. The type of molecular film covering a surface has a dramatic influence on the surface forces and mechanical properties of the interface. In particular, a polar alcohol end-group on the linear perfluoropolyether polymer increases the contact pressure that a liquid lubricant film can support, thereby providing a beneficial effect by preventing solid-solid contact. Many of the descriptions developed using macroscopic continuum mechanics analysis are still applicable to these atomic-scale contact zones. However, complete interpretation of the results requires extension of the continuum mechanics analysis to include descriptions of the atomic and molecular processes.

Fomblin is a registered trademark of Ausimont, S.p.A., Milan, Italy.

References

- G. Binnig, C. F. Quate, and Ch. Gerber, "Atomic Force Microscope," Phys. Rev. Lett. 56, 930 (1986).
- J. A. Greenwood and J. B. P. Williamson, "Contact of Nominally Flat Surfaces," Proc. Roy. Soc. Lond. A 295, 300 (1966).
- J. A. Greenwood and J. H. Tripp, "The Elastic Contact of Rough Surfaces," Trans. ASME E, J. Appl. Mech. 34, 153 (1967).
- 4. J. A. Greenwood, "The Area of Contact Between Rough Surfaces and Flats," *Trans. ASME F* 89, 81 (1967).
- F. P. Bowden and D. Tabor, The Friction and Lubrication of Solids, Oxford University Press, New York, 1950.
- D. Tabor, "The Role of Surface and Intermolecular Forces in Thin Film Lubrication," Microscopic Aspects of Adhesion and Lubrication, J. M. Georges, Ed., Tribology Series 7, Flsevier, New York, 1982, pp. 651-682
- Series 7, Elsevier, New York, 1982, pp. 651-682.
 A. M. Homola, J. N. Israelachvili, M. L. Gee, and P. M. McGuiggan, "Measurement of and Relation Between the Adhesion and Friction of Two Surfaces Separated by Molecularly Thin Liquid Films," Trans. ASME, J. Tribol. 111, 675 (1989).
- A. M. Homola, J. N. Israelachvili, P. M. McGuiggan, and M. L. Gee, "Fundamental Experimental Studies in Tribology: The Transition from 'Interfacial' Friction of Undamaged Molecularly Smooth Surfaces to 'Normal' Friction," Wear 136, 65 (1990).
- C. M. Mate, G. M. McClelland, R. Erlandsson, and S. Chiang, "Atomic-Scale Friction of a Tungsten Tip on a Graphite Surface," Phys. Rev. Lett. 59, 1942 (1987).
- D. Rugar, H. J. Mamin, and P. Guethner, "Improved Fiber-Optic Interferometer for Atomic Force Microscopy," Appl. Phys. Lett. 55, 2588 (1989).
- Microscopy," Appl. Phys. Lett. 55, 2588 (1989).
 S. Alexander, L. Hellemans, O. Marti, J. Schneir,
 V. Elings, P. K. Hansma, M. Longmire, and J. Gurley,
 "An Atomic-Resolution Atomic-Force Microscope
 Implemented Using an Optical Lever," J. Appl. Phys. 65, 164 (1989).
- G. Meyer and N. M. Amer, "Simultaneous Measurement of Lateral and Normal Forces with an Optical Beam Deflection Atomic Force Microscope," Appl. Phys. Lett. 57, 2089 (1990).
- G. S. Blackman, C. M. Mate, and M. R. Philpott, "Interaction Forces of a Sharp Tungsten Tip with Molecular Films on Silicon Surfaces," *Phys. Rev. Lett.* 65, 2270 (1990).
- C. M. Mate and V. J. Novotny, "Molecular Conformation and Disjoining Pressure of Polymeric Liquid Films," J. Chem. Phys. 94, 8420 (1991).

- 15. J. B. Pethica and W. C. Oliver, "Tip Surface Interactions in STM and AFM," *Phys. Scripta T* 19, 61 (1987).
- N. A. Burnham and R. J. Colton, "Measuring the Nanomechanical Properties and Surface Forces of Materials Using an Atomic Force Microscope," J. Vac. Sci. Technol. A 7, 2906 (1989).
- N. A. Burnham, R. J. Colton, and H. M. Pollock, "Interpretation of Force Curves in Force Microscopy," Nanotechnol. 4, 64 (1993).
- J. N. Israelachvili, Intermolecular and Surface Forces with Applications to Colloidal and Biological Systems, Academic Press, Inc., New York, 1985.
- N. A. Burnham, D. D. Dominguez, R. L. Mowery, and R. J. Colton, "Probing the Surface Forces of Monolayer Films with an Atomic Force Microscope," *Phys. Rev. Lett.* 64, 1931 (1990).
- R. Erlandsson, G. Hadziionnou, C. M. Mate, G. M. McClelland, and S. Chiang, "Atomic Scale Friction Between Muscovite Mica Cleavage Plane and a Tungsten Tip," J. Chem. Phys. 89, 5190 (1988).
- S. Akamine, R. C. Barrett, and C. F. Quate, "Improved Atomic Force Microscope Images Using Microcantilevers with Sharp Tips," *Appl. Phys. Lett.* 57, 316 (1990).
- G. J. Germann, S. R. Cohen, G. Neubauer, G. M. McClelland, and H. Seki, "Atomic Scale Friction of a Diamond Tip on Diamond (100) and (111) Surfaces," J. Appl. Phys. 73, 163 (1993).
- I. P. Batra and S. Ciraci, "Theoretical Scanning Tunneling Microscopy and Atomic Force Microscopy Study of Graphite Including Tip-Surface Interactions," J. Vac. Sci. Technol. A 6, 313 (1988).
- F. F. Abraham and I. P. Batra, "Theoretical Interpretation of Atomic Force Microscope Images of Graphite," Surf. Sci. 209, L125 (1989).
- W. Zhong and D. Tomanek, "First Principles Theory of Atomic Scale Friction," Phys. Rev. Lett. 64, 3054 (1990).
- G. Overney, W. Zhong, and D. Tomanek, "Theory of Elastic Tip-Surface Interactions in Atomic Force Microscopy," J. Vac. Sci. Technol. B 9, 479 (1991).
- S. A. C. Gould, K. Burke, and P. K. Hansma, "Simple Theory for the Atomic Force Microscope with a Comparison of Theoretical and Experimental Images of Graphite," *Phys. Rev. B* 40, 5363 (1989).
- K. L. Johnson, Contact Mechanics, Cambridge University Press, Cambridge, England, 1985, Ch. 7.
- J. B. Pethica, "Comment on Interatomic Forces in Scanning Tunneling Microscopy: Giant Corrugation of the Graphite Surface," Phys. Rev. Lett. 57, 3235 (1986).
- C. M. Mate, "Atomic Force Microscopy of Polymer Lubricants on Silicon Surfaces," Phys. Rev. Lett. 68, 3323 (1992).
- M. Binggeli and C. M. Mate, "Influence of Capillary Condensation of Water on Nanotribology Studied by Force Microscopy," Appl. Phys. Lett. 65, 415 (1994)
- Force Microscopy," Appl. Phys. Lett. 65, 415 (1994).
 32. H.-W. Hu, G. A. Carson, and S. Granick, "Relaxation Time of Confined Liquids Under Shear," Phys. Rev. Lett. 66, 2758 (1991).
- J. Van Alsten and S. Granick, "Molecular Tribometry of Ultrathin Liquid Films," Phys. Rev. Lett. 61, 2570 (1988).
- M. L. Gee, P. M. McGuiggan, and J. N. Israelachvili, "Liquid to Solidlike Transition of Molecularly Thin Films Under Shear," J. Chem. Phys. 93, 1895 (1990).
- A. M. Homola, H. V. Nguyen, and G. Hadziioannou, "Influence of Monomer Architecture on the Shear Properties of Molecularly Thin Polymer Melts," J. Chem. Phys. 94, 2346 (1990).
- R. M. Overney, E. Meyer, J. Frommer, D. Brodbeck,
 R. Luthi, L. Howald, H.-J. Guntherodt, M. Fujihira, H.
 Takano, and Y. Gotoh, "Friction Measurements on Phase Separated Thin Films with a Modified Atomic Force Microscope," Nature 359, 133 (1992).

- R. M. Overney, E. Meyer, J. Frommer, H.-J. Guntherodt, M. Fujihira, H. Takano, and Y. Gotoh, "Force Microscopy Study of Friction and Elastic Compliance of Phase-Separated Organic Thin Films," *Langmuir* 10, 1281 (1994).
- R. M. Overney, T. Bonner, E. Meyer, M. Ruetschi,
 R. Luthi, L. Howald, J. Frommer, M. Fujihira, and
 H. Takano, "Elasticity, Wear, and Friction Properties of Thin Organic Films Observed with Force Microscopy,"
 J. Vac. Sci. Technol. B 12, 1973 (1994).

Received November 10, 1994; accepted for publication July 18, 1995

C. Mathew Mate IBM Research Division, Almaden Research Center, 650 Harry Road, San Jose, California 95120 (MATE at ALMADEN, mate@almaden.ibm.com). Dr. Mate is a research staff member in the Storage Systems and Technology Department at the Almaden Research Center. He received a B.S. degree in engineering physics in 1981 and a Ph.D. in physics in 1986, both from the University of California at Berkeley. Since joining IBM Almaden in 1986, he has used atomic force microscopy to elucidate the atomic-level origins of friction, lubrication, and wear, and has studied tribology issues related to disk drive development. In 1990, he received an IBM Research Division Award for advances in scanning tunneling microscopy and, in 1992, an IBM Outstanding Technical Achievement Award for his work on lubrication in disk drives. Dr. Mate is a member of the American Physical Society, the American Chemical Society, the American Vacuum Society, and the Materials Research Society.